LOAD REGULATION OF POWER PLANTS

Fossil-fuel-driven steam-electric power plants may operate as both load-following and baseload units. Load-following operations require careful monitoring and control of plant variables with due consideration to plant stability and performance constraints. Power plant performance is usually expressed in terms of thermodynamic efficiency during steady-state operations and load regulation to match actual load demand under transient operations. An often overlooked problem under load regulation and rapid power maneuvering is the impact of load variation on service life, that is, structural durability, of power plant components. Under transient operations such as load following and start-up, the critical plant components are subjected to high thermal and mechanical stresses due to variations in steam temperature, pressure, and flow rate with the attendant risk of significant reduction in the service life (1). For example, a plant with 40 years of useful life is usually recommended for up to 100 cold starts and emergency shutdowns as an indicator of allowable limits of severe operational transients. Therefore, while matching the varying load demand on a day-to-day or even an hourly basis, power plants need to be operated in an optimal manner to avoid premature component failures and forced plant shutdowns. The obvious benefits include increased service life of plant components, increased availability, and cost reduction.

This article introduces a new technique called life-extending load-following control (LELFC) for power plants. The objective here is to maximize the service life of fossil power plants under load regulation without compromising the required plant performance. Essentially life extension is achieved through reduction in structural damage to plant components that can occur in ways such as fatigue and creep crack growth and through corrosion. Ray et al. (2,3) and Dai and Ray (4) have introduced the concept of damage-mitigating control of complex thermomechanical systems with a specific example of a reusable rocket engine. The technical approach is interdisciplinary, relying on:

- Mechanics of materials, along with thermodynamics and fluid mechanics, to develop models of power plant dynamics and structural damage in critical plants
- Systems-theory and approximate reasoning, to design a hierarchically structured robust control strategy based on the above models

Structural damage occurs due to excessive temperature and pressure oscillations during transient conditions (5). The plant performance criterion is expanded to include temperature and pressure oscillations at critical plant components. Kallappa et al. (5) and Kallappa and Ray (6) have taken this approach to design a LELFC system for power plant load regulation while achieving life extension. The issues of robust stability and performance are also addressed. The LELFC system, presented in this article, is designed for performance–damage trade-off under wide range operations from 25% to 100% of the rated plant load. The control strategies are synthesized using mathematical models of power plants (7) and structural damage processes (5) in the state-variable setting. Implementation of these strategies in an operating power plant would require a state-variable plant model which matches, at the very least, with the steady-state input–output characteristics of the actual plant. The uncertainty modeling techniques for robust controller design (8), can be used to overcome some limitations arising from mismatch during transient operations.

The next section discusses the basic framework of a control system for a steam-electric fossil power plant which must respond to load demands and enhance component life and plant availability. The sections that follow introduce different tools for achieving the design goals. The control tools introduced are followed by simulation experiments which demonstrate the effectiveness of these tools.

LIFE-EXTENDING LOAD-FOLLOWING CONTROL SYSTEM

The goal of a life-extending load-following control (LELFC) system is to formulate feedforward-feedback control law(s) in order to satisfy the performance objective(s), while maintaining the damage accumulation and damage rate within prescribed limits. A major benefit of the LELFC system is to facilitate daily cycling of large generating units that might have been originally designed for baseload operations only. This process takes advantage of: (i) constrained nonlinear optimization for feedforward control; (ii) robust linear analysis and synthesis tools for feedback control; and (iii) approximate reasoning (i.e., fuzzy logic) for hierarchically structured decision-making. The major challenge in the synthesis of LELFC systems is to account for the nonlinear characteristics of thermal-hydraulic dynamics of the power plant process and material damage in the structural components.

In general, a combination of feedforward control (FFC) and feedback control (FBC) is needed for wide-range operation of fossil power plants (7). The FFC policy does not have the ability to compensate for disturbances and plant modeling uncertainties. That is, under FFC alone, the plant outputs may drift away from the desired trajectory. On the other hand, FBC alone is often inadequate for wide-range control of nonlinear plant dynamics. These problems can be remedied by using a combination of feedback and feedforward control. While a robust feedback control is necessary to overcome perturbations in the plant dynamics, an open-loop feedforward policy provides a nominal trajectory that reduces feedback control efforts and improves the overall performance. In this article the load regulation FFC laws are developed to handle two scenarios. The first one is where the operating strategy is known a priori and the other where it is not. A priori knowledge of the operating strategy can be used to formulate a

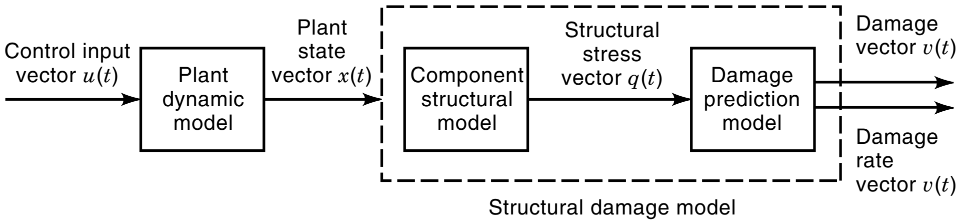

Figure 1. Damage prediction/estimation system. For individual plant components, separate structural damage models are needed. For on-line operations, the plant dynamic model is replaced by the actual plant.

feedforward strategy which takes into account directly the damage rate and accumulation.

One of the tools for LELFC design is the damage-prediction system shown in Fig. 1 for quantitative estimation of structural damage in components. The plant model is a finite-dimensional state-space representation of the power plant dynamics under control. The plant states (or their estimates) are inputs to the component structural model which generates the necessary information for the damage-prediction model. The output of the structural model is the *structural stress vector* which, for example, consists of time-dependent stress, strain, and temperature at critical point(s) of the structure (e.g., main steam and hot reheat headers, or superheater and reheater tubes in steam generators). The damage model is a continuous-time representation of material degradation so that this model can be integrated with the plant dynamic model in the state-variable setting. The objective here is to include the effects of time-dependent damage rate and damage accumulation at the critical points of plant components which are subjected to time-dependent, varying-amplitude load. The damage state vector $\boldsymbol{v}(t)$ indicates the damage levels, for example, in terms of fatigue cracks and inelastic strain due to thermomechanical fatigue and creep-plasticity. The time derivative of damage, $\dot{\boldsymbol{v}}(t)$ indicates how the instantaneous load is affecting the critical structure(s) of the plant.

The structural damage model is highly nonlinear as are the actual damage phenomena. Therefore it is difficult to control damage solely by linear feedback control. Damage mitigation requires an understanding of the causal relationships between various plant conditions and damage rate. This knowledge is useful for mitigating the damage rate through control of these plant conditions. The component structural model and the damage model are derived by applying the fundamental principles of thermodynamics and mechanics to creep and plastic deformation and fatigue crack growth. The damage model generates both damage rate and accumulation as continuous functions of time.

A general structure of the plant and damage models used in the LELFC system follows. All representations are in continuous time-invariant state-space setting.

Plant dynamics:

$$\begin{aligned} \dot{\boldsymbol{x}} &= f(x,u)\forall t \geq t_0 \qquad \text{given } x(t_0) = x_0 \\ \boldsymbol{y} &= g(x,u) \end{aligned} \tag{1}$$

Damage dynamics:

$$\dot{\boldsymbol{v}} = h[v, q(x,u)] \qquad \text{such that } h \geq 0\, \forall t \geq t_0 \qquad \text{given } v(t_0) = v_0 \tag{2}$$

where $\boldsymbol{x} \in R^{\mathrm{n}}$ and $\boldsymbol{y} \in R^{\mathrm{p}}$ are the plant state and plant output vectors;

$\boldsymbol{u} \in R^{\mathrm{m}}$ is the control input vector

$\boldsymbol{v} \in R^{\ell}$ is the damage state vector

$\boldsymbol{q} \in R^{\mathrm{r}}$ is the structural stress vector

Damage is a structural degradation process which leads to reduction in functional life of the component, for example, cracks, corrosion, creep and plastic deformation. Critical components in a fossil-fuel power plant which limit its functional life include:

- Turbine rotor bearings, shaft, and casing, which fail due to vibrations and friction damage
- Steam generator tubes that fail due to creep and corrosion
- Main steam and hot reheat steam headers that fail due to creep–fatigue interaction.

This article focuses on life extension of main steam and hot reheat steam headers and the radiant superheater and reheater sections of steam generator tubes. The rationale for selection of these components for life extension of the power plant is that together they constitute the major source of forced shutdown (9). Modeling of damage in steam headers and steam generator tubes is discussed in detail by Kallappa et al. (5) and Lele et al. (10), respectively. Note that other mathematical models can be used for control synthesis, provided that these are sufficiently accurate and computationally tractable. The control strategies suggested here can be used to reduce damage in other plant components too.

The LELFC system consists of three modules or systems, as shown in Fig. 2. These modules together calculate the in-

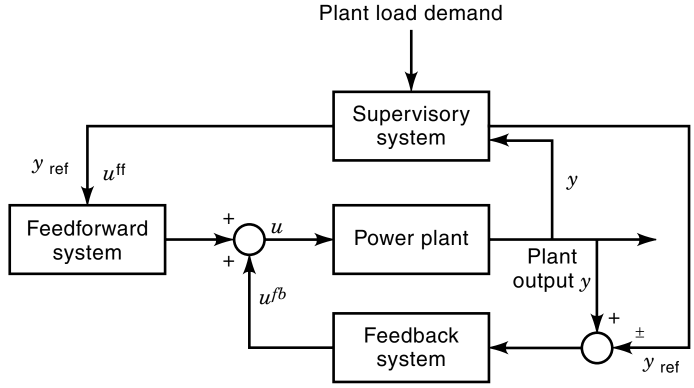

Figure 2. Structure of control system.

put to the plant. As shown in Fig. 2, the system uses a combination of feedforward (u^{ff}) and feedback (u^{fb}), to form vector u ($u = u^{ff} + u^{fb}$). The measured plant output vector is denoted by y and the plant output reference signal is denoted by y_{ref}. The control system is managed by a supervisory system, which receives the load demand from a remotely located automatic dispatch system (ADS). The goals of the complete control system, composed of the feedforward, feedback, and supervisory systems, are as follows:

1. Load following by taking the plant load (MWe) starting from a steady-state level to the target point within the prescribed time
2. Maintaining plant stability and performance robustness in the presence of sensor noise and modeling uncertainties
3. Maintaining steam temperatures and pressures within a prespecified range to mitigate structural damage in plant components

There is clearly a trade-off between achieving goal 1 and the remaining two goals.

The control systems are tested via simulation experiments on a once-through steam power plant model with a rated capacity of 525 MWe. The plant dynamics are represented by a 27th-order nonlinear state-space model, which is described in detail by Weng, Ray, and Dai (7). The plant maintains the throttle steam condition at 2415 psia and 950°F and hot reheat steam temperature at 1000°F for loads over 40%. At lower loads the throttle pressure needs to be lowered. Goal 3 is achieved by maintaining these three conditions as such. The following four valve commands are selected as control inputs: (1) high-pressure turbine governor valve area (AGVR), (2) feedpump turbine control valve area (APTR), (3) furnace fuel/air valve area (AFAR), and (4) reheat spray attemperator valve area (AATR). The measured plant outputs are electric power (JGN in MWe), throttle steam temperature (THS), hot reheat steam temperature (THR), and throttle steam pressure (PHS). All simulations and examples are specific to this plant.

The next three sections discuss in detail the various aspects in the design of the three systems and present some simulation results. The three systems can be synthesized and used independently of each other, but, as simulation results will show, they produce better results when used in conjunction with each other.

FEEDFORWARD SYSTEM DESIGN

The feedforward system objective is to maneuver the plant from an initial equilibrium state to a new equilibrium state within a specified time and without violating the prescribed physical and damage constraints. The motivation here is to facilitate daily cycling of large electric generating units. Input to the feedforward system is always the current desired load output in MWe (y_{ref} in Fig. 2) and its output is the current command signal to position the input valves (u^{ff}) in the absence of any feedback.

During steady-state operation u^{ff} is held constant at the steady-state value of the command input corresponding to the steady-state outputs. Under steady-state operations the plant states and inputs are determined by the load and other outputs (pressure and temperatures). Following Eq. (1), the steady-state condition is defined as:

$$f(x_{ss}, u_{ss}) = 0 \qquad \text{and} \qquad y_{ss} = g(x_{ss}, u_{ss}) \tag{3}$$

where the subscript "ss" denotes steady state. The steady-state inputs and states are obtained by solving Eq. (3) for u_{ss} and x_{ss} for a desired output y_{ss}. Since u_{ss} and x_{ss} are uniquely determined by y_{ss} the damage rate and performance are also unique for a given steady-state operating condition of load demand, steam pressure, and temperature. On the other hand, during transient operations each input of the power plant can be changed in different ways to the dual objectives of load following and damage mitigation.

Damage in power plant components can be severe during transients such as start-up, shutdown, and load-following operations (11) because of fluctuations in steam temperatures, pressures, and other state variables. If the operation strategy is known a priori, a damage-mitigating feedforward policy can be formulated via off-line optimization based on the damage-prediction systems. The cost functional for this optimization is a weighted sum of the measures of plant performance and accumulated structural damage. If the operational strategy is not known a priori, on-line optimization is required. This may not be practical due to computational limitations. Therefore feedforward for this case is determined by y_{ref}, the reference output, based on the steady-state operations and Eq. (3). The u^{ff} for each y_{ref} corresponds to the steady-state input for the output. This u^{ff} is not damage mitigating.

An optimal feedforward control (FFC) policy can be generated as an input sequence over a finite-time horizon to enable rapid response to changes in load demand. The performance index is expressed in terms of the deviation from the desired load temperatures and pressure, and the rate of change of actuator commands. The objective is to minimize a nonlinear cost functional which represents the plant performance, damage accumulation without violating given damage, and damage rate constraints along with performance constraints (operating temperatures and pressures).

The optimal FFC is synthesized via constrained nonlinear programming (NP) due to the nonlinear plant and damage models. Since optimization of FFC is computationally expensive due to the large models used, on-line methods of optimization, such as receding horizon predictive control, appear to be ineffective. Therefore optimal FFC is generate off-line with feedforward actuator valve positions (u^{ff}) being the decision variables. A quadratic cost functional is chosen as the sum of the square of weighted deviation of plant outputs and control effort (change in input valve positions) and weighted absolute value of the damage rate and damage accumulation which are nonnegative. The optimization procedure identifies a finite sequence of control inputs $\{u_k\}_{k=0}^{N-1}$ at uniform time steps for $k = 0$ to $N - 1$ that will minimize this functional. Since each of the plant and damage models has a continuous-time structure, the control inputs are, in effect, continuous-time steps where u_k represents the height of the step for the duration $[t_k, t_{k+1})$. The sequence of control inputs are calculated such that the plant can be maneuvered from a known initial plant state x_o and damage state v_o at initial time t_o close to the specified terminal state and control effort at the final time t_f corresponding to the final time step N. The optimization procedure is summarized below:

Minimize:

$$J = \sum_{k=0}^{N-1}[\tilde{y}_{k+1}^T Q_{k+1}\tilde{y}_{k+1} + \tilde{u}_k^T R_k \tilde{u}_k + S_k v_k^{\acute{Y}}] + \sum_{i=1}^{\mathbf{L}}(v_{Ni} - v_{oi}) \quad (4)$$

Subject to the following constraints:

Plant dynamics:

$$x_{k+1} = x_k + \int_{t_k}^{t_{k+1}} f[x(t), u(t)]\,dt \qquad x_k|_{k=0} = x(t_0) = x_0 \quad (5)$$

Plant output: $\quad y_k = g(x_k, u_k) \quad$ (6)

Control signal bound: $\quad 0 \le u_k^i < \alpha^i \qquad i = 1, 2, \mathbf{L} \qquad m \quad$ (7)

Plant output constraints: $\quad |\tilde{y}_k^i| < \gamma_k^i \qquad i = 1, 2, \mathbf{L} \qquad p \quad$ (8)

Damage rate: $\quad 0 \le \acute{v}_k^i < \beta_k^i \qquad i = 1, 2, \mathbf{L} \qquad \mathbf{L} \quad$ (9)

Damage accumulation: $\quad v_N^i - v_0^i < \Gamma^i \qquad i = 1, 2, \mathbf{L} \qquad \mathbf{L} \quad$ (10)

where

x_k, u_k, and y_k are plant states, control inputs, and plant outputs, respectively, at time t_k

$\tilde{y}_k = y_k - \hat{y}_k$ is the deviation of the actual output from the desired output

$\tilde{u}_k = u_k - u_{k-1}$ is the incremental change in the control input at time t_k

v_k is the damage state

$\acute{v}_k^i$ is the damage rate

N is the total number of discrete time steps for the time period $[t_0\ t_f]$

$Q_k \in R^{p\times p}$; $R_k \in R^{m\times m}$ and $S_k \in R^{1\times L}$ are weighting matrices, $k = 1, L, N$

α^i is the normalized upper limit of the ith actuator position vector

β_k^i is the maximum rate of the ith damage state vector at time t_k

γ_k^i is the normalized constraint for the ith output deviation $\tilde{y}_k^i$ at time t_k

Γ^i is the maximum increment of the ith damage state for the time period $[t_0\ t_f]$

Figure 2 shows implementation of the optimal FFC by the feedforward system. The control input u to the plant is composed of the addition of two signals. The first is the feedforward signal, u^{ff}, and the second is the feedback signal, u^{fb}. Prior to initiation of the transients (e.g., load ramp up), u^{ff} is held at the steady-state value of the inputs corresponding to the initial load. During transients, u^{ff} is identically equal to the optimal FFC which is generated off-line via constrained optimization over a specified finite interval of time. At the expiration of the finite time interval, u^{ff} is held at the steady-state value corresponding to the inputs at the final load. The feedback signal, u^{fb}, is provided on-line by the feedback controller. To maintain robustness at all times the linear feedback system is active during both steady-state and transient conditions. The presence of a feedforward during transient operations reduces the feedback control effort and damage.

SIMULATION EXAMPLES FOR FEEDFORWARD SYSTEM

Optimal feedforward control policies were obtained for the given plant model with actuator and plant output constraints for the transient operations of load following. Only the case of power ramp-up under normal operating conditions is presented as a typical example in this article. During the ramp-up operation, the plant load (JGN) was uniformly increased from 40% to 100% base load, that is, from 210 MWe to 525 MWe, in 360 s. The main steam header pressure (PHS) was constrained within ±45 psia around the nominal value of 2415 psia. Similarly, the main steam temperature (THS) was constrained within ±10°F around the nominal value of 950°F and the hot reheat steam temperature (THR) within ±15°F around the nominal value of 1000°F. For the feedforward experiments only the main steam header damage was taken into account. Damage to other components can also be included in the optimization, but that would make the optimization computationally intensive. The goal is to demonstrate the effectiveness of the optimization and it can be done by using just one critical component.

Before this optimization study was conducted, simulation experiments were conducted for the above ramp-up operation based on an ad hoc feedforward input trajectory which is often practiced in industry (1). The objective was to observe the accumulated damage level and damage rate for this power-ramping operation. The ad hoc feedforward input trajectory was constructed by uniformly interpolating between steady-state input values for 40% and 100% load. The observed damage levels and damage rates were used as constraints during nonlinear optimization to calculate the optimal feedforward trajectory.

The FFC sequence was updated at a uniform interval of 1 s (i.e., $t_k - t_{k-1} = 1$ s for $k = 1, 2, \ldots, N$). With four control inputs at each time step, the number of decision variables, $\{u_k\}_{k=0}^{N-1}$, is 1440 for a period of 360 s. The decision vector, $u_k = \{\mathrm{AGV}_k, \mathrm{APT}_k, \mathrm{AFA}_k, \mathrm{AAT}_k\}^{\mathrm{T}}$ is the vector of normalized valve positions varying from 0 (fully closed) to 1 (fully open). Other details of these simulations are described in Ref. 5.

Upon completion of the optimization task, simulation runs were conducted for two different scenarios, each for a mid-life operation of the plant for a period of 9000 s. Each of these simulation experiments started with a ramp-up operation (duration 360 s) followed by a steady-state operation around 100% load for 8640 s. The simulation are used to demonstrate the superiority of the optimized feedforward trajectory over the ad hoc trajectory.

The first scenario used the ad hoc input feedforward sequence for the ramp-up followed by the steady-state values of the control inputs. The second scenario used the optimal feedforward control sequences, instead of the ad hoc ones, for the ramp-up operation and maintained the steady-state control inputs for feedforward thereafter. Feedback control was used in these simulations. Its design will be discussed in the subsequent section. The same feedback system was used for both simulations, to have a fair comparison between the two types of feedforward.

Figures 3 and 4 compare the results of simulations obtained from the ad hoc feedforward control and the optimized feedforward control. Figure 3 shows that the overall performance of the optimized feedforward sequence is clearly superior to that of the ad hoc feedforward sequence. The output in

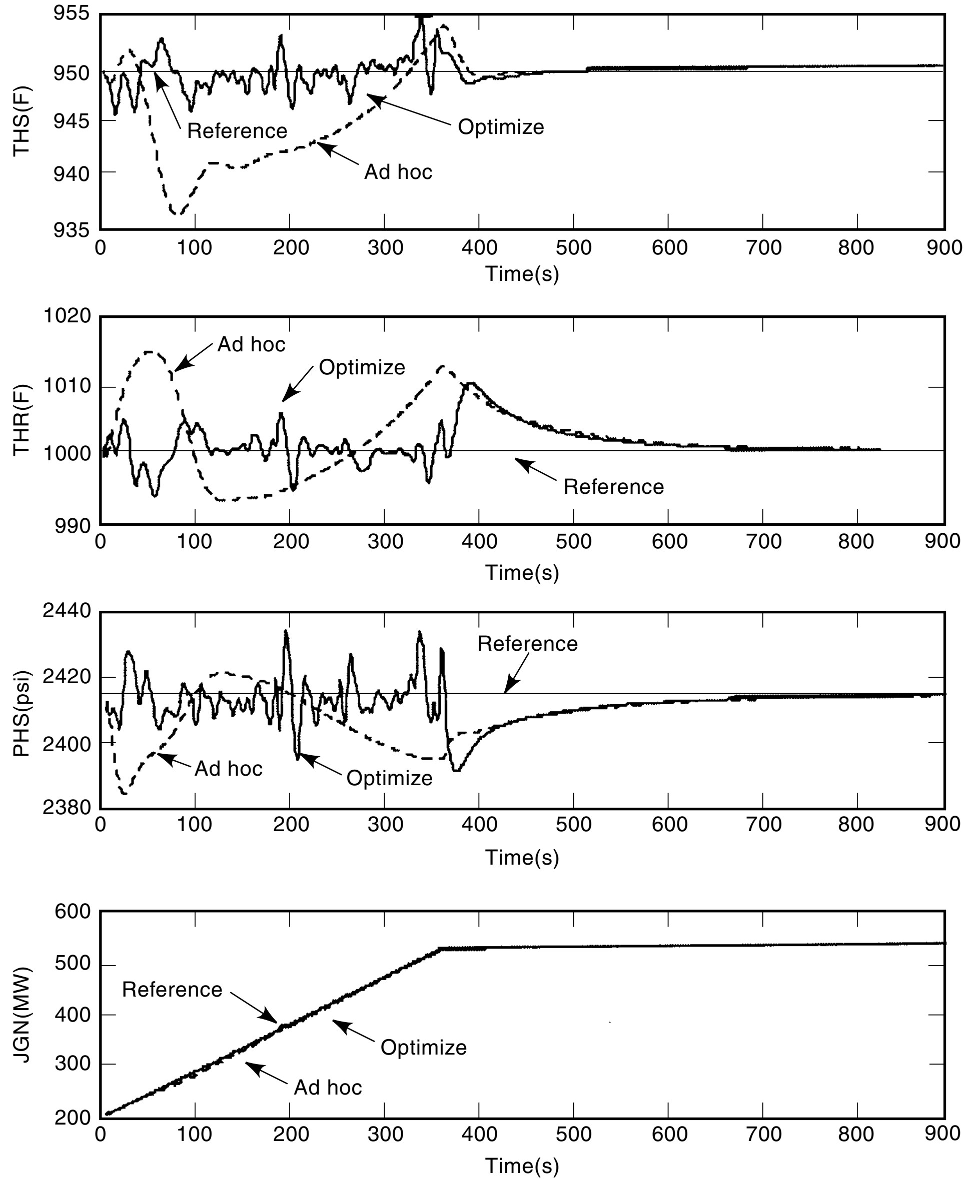

Figure 3. Performance comparison between ad hoc and optimized feedforward. This figure represents performance during power ramp up from 40% to 100%, beginning at zero seconds and ending at 360 seconds at a ramp rate of 10% per minute. The amplitude of temperature and pressure variations are smaller for optimized feedforward. This improvement is achieved with a slight reduction in JGN performance and helps reduce damage as seen in Fig. 4.

the optimized feedforward case follows the reference load (JGN) trajectory more closely. (It is difficult to distinguish the two load trajectories from the plot due to scaling.) Furthermore, although the temperature and pressure signals in the optimized case have higher frequency contents due to more rapid maneuvering of the control valves, they have smaller amplitude than in the ad hoc case. For each plant output, steady-state is reached at approximately the same time. The optimal trajectory generation is driven by three goals: first, to follow the output ramp as closely as possible, which is demonstrated in Fig. 3; second, to keep the three other outputs within specified bounds, for safety reasons and damage mitigation. Figure 3 demonstrates that the optimized feedforward keeps the outputs within bounds and relatively closer to the reference output, as compared to the ad hoc input. The third aim is to reduce damage due to creep and fatigue in the steam headers. Both creep and fatigue damage are functions of the steam temperature and pressure. The optimization process keeps a trade off between load-following and safety and damage constraints.

Figure 4 compares the damage and damage rates resulting from the plant operation and control scenarios of Fig. 3. Fatigue damage accumulation and rate are calculated by the fatigue crack growth model in terms of the increments of crack length in mm, assuming an initial crack length of 1.5 mm. Creep damage is expressed as a normalized dimensionless variable. It is the reduction in thickness of the header pipe divided by the original thickness. In effect, creep and fatigue damage accumulations and rates shown in Fig. 4 refer to the thinning and cracking of the main steam header. Both fatigue and creep damage are lower for the optimized input as compared to the ad hoc input. For both types of damage, under the ad hoc feedforward control inputs, the peak occurs during the transient condition of power ramp-up. This demonstrates the need for damage mitigation during transient operations. The life-extending load-following under the optimized feedforward inputs reduces the creep thinning damage by about 40% and the fatigue damage by about 90%, as seen in Fig. 4. Optimal feedforward control achieves significant savings in structural damage, as compared with ad hoc feedforward. How-

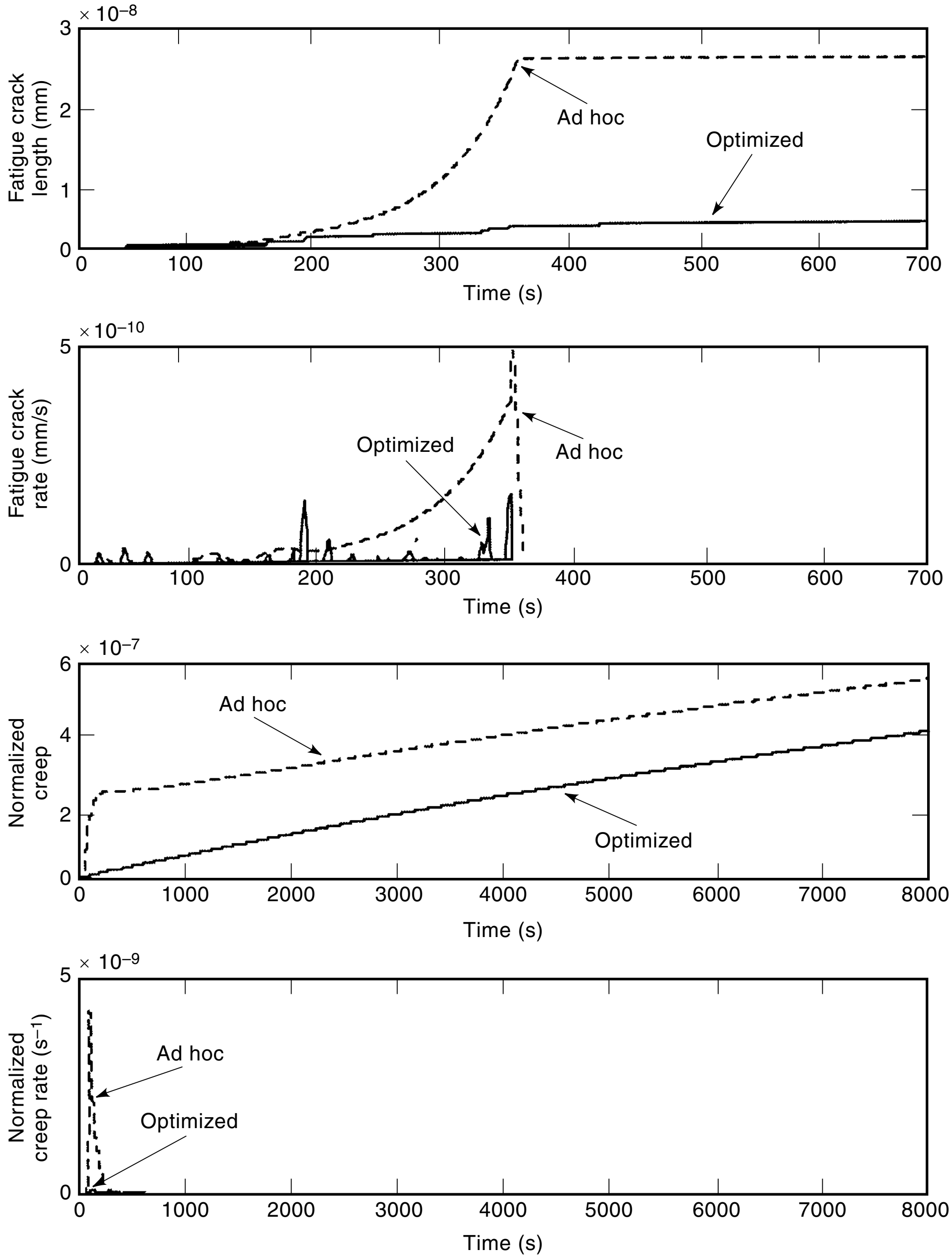

Figure 4. Damage comparison between ad hoc and optimized feedforward. Damage accumulation and rate correspond to operations represented in Fig. 3. Optimized feedforward results in lower damage and damage rates.

ever, this requires rapid maneuvering of the control valves, which will increase wear and therefore more frequent maintenance of actuator valves will be needed. This is a small price in contrast to the gain achieved by life extension of the steam header and (possibly) other plant components such as steam generators and steam turbines.

FEEDBACK SYSTEM DESIGN

The feedback signal u^{fb} is provided on-line by the feedback controller. Controller synthesis is done, keeping in mind not only the desired plant performance but also the effect of various states on damage of critical plant components. The control objectives include manipulation of these states to reduce damage. In effect, the feedback controller is a damage-mitigating controller which is designed to be robust and to handle plant disturbances, modeling uncertainties, and sensor noise.

The mathematical tools needed to design nonlinear controllers are not sufficiently developed to handle systems as large as a complete power plant. Therefore linear controller synthesis techniques are used. The feedback controller is synthesized based on linearized plant model(s). To circumvent the problem of large perturbation under wide-range operation, a set of feedback controllers are designed and implemented via gain scheduling (12), which is implemented by the supervisory system. The feedback control (FBC) system is designed in the sample-data configuration in which the sampler and hold are synchronized, as seen in Fig. 5. That is, even though the computation of the feedback signal $u(k)$ is completed before expiration of the sampling period, it is held in the buffer until the beginning of the next sample. This synchronization with the sampler makes implementation easier and should not cause any appreciable performance degradation if the sampling period, T, is chosen small relative to the process dynamics. Having the sampler and hold synchronized

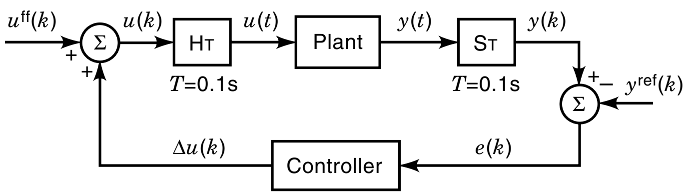

Figure 5. Feedback control system configuration. The plant operates in continuous time while the controller operates in discrete time. In the Sample Data Controller configuration, H_T is the hold timer and S_T is the sample timer.

allows the use of a powerful sampled data feedback controller design technique. This technique takes advantage of the fact that a synchronized sampled-data system is T-periodic, since shifting the system inputs by an integer multiple of T will result in the plant outputs being sampled at the same points, but shifted by the multiple of T. For the power plant considered in this article, a sample time of 0.1 s was found to be sufficient for control purposes. Unlike a discrete controller, the sample data technique also guarantees intersample performance.

A feedback controller synthesis technique has been adopted, which minimizes the worst-case gain between the energy of exogenous inputs (e.g., noise, disturbances, and reference signals) and regulated outputs (e.g., error signals and control effort). This is known as L_2-induced controller synthesis which involves finding the stabilizing controller K which minimizes:

$$\|T_{zw}(K)\|_{L_2-ind} = sup \left\{ \frac{|z|_{L_2}}{\|w|_{L_2}} \middle| \|w\|_{L_2} \neq 0 \right\} \tag{11}$$

where T_{ZW} is the closed-loop transfer function between the previously mentioned exogenous inputs (w) and exogenous outputs (z), and $\|\cdot\|_{L_2}$ denotes a norm whose value is the energy of the signal that it operates on. For linear time invariant systems, controller synthesis based on the induced L_2-norm is known as H_∞ controller synthesis, which has been well documented in the control literature (13). However, H_∞ controller synthesis cannot be applied directly to sampled-data systems because of their time varying nature. Bamieh and Pearson (14) proposed a solution to the L_2-induced controller synthesis problem for sampled-data systems, which has subsequently been incorporated as the function *sdhfsyn* in the MATLAB *mutools* toolbox (15).

Since the linear model being used for the synthesis of the feedback controller is only an approximation of the true dynamics of the power plant, the designed controller should exhibit robustness properties. Analysis of the robust stability and performance of sampled data systems has been explored in a paper by Sivashankar and Khargonekar (16). For controller synthesis, a *D-K* iteration technique toolbox (17) can be used where "suboptimal" rational polynomial weights *D*'s are found using μ-synthesis and the controller K is found using the induced L_2 sampled-data design procedure.

In a wider range of power plant operation from 25% to 100% of full load, a single linear feedback controller does not yield required performance or stability because the plant dynamics are very nonlinear in the lower range. The single controller is designed on a given linearized plant model using linear techniques and may not meet the stability and performance requirements while operating away from the linearization point. Analogous to plant stability and performance, the damage-mitigation quality of a control system may not be effective if away from the postulated region of plant operation. Gain scheduling is commonly used for wide-range control of complex dynamical processes such as power plants and tactical aircrafts. It allows robust linear control of (continuous) nonlinear plants over a wide operating range. It breaks the task of control synthesis into two steps (17).

The first step is to synthesize a family of local linear controllers based on linearization of the nonlinear plant at several different equilibrium points (operating conditions). The linear controllers yield satisfactory local performance, that is, when the nonlinear plant is operated near the respective operating points. The second step involves interpolation of the linear control laws at intermediate operating conditions. The role of a gain-scheduling policy is to schedule the gains/parameters of the linear control law structure. This scheduling is dependent on the operating conditions. One or more of the operating conditions could form the independent scheduling variable. Major issues in the gain-scheduling decision include the number of linear controllers, the algorithm for switching from one controller to another, and the choice of the scheduling variable. These choices are to be made with due consideration to stability, performance, life extension, and overall cost.

The optimal number of gain-scheduled controllers should take into account two factors: (1) robust stability and performance in the entire operating range; and (2) impact of switching transients or interpolation of control signals on the plant performance. Although an increase in the number of controllers in the operating range often improves the performance, any switching action may lead to an abrupt change in the closed-loop plant dynamics and the occurrence of such phenomena should be kept minimal. The number of controllers may differ from plant to plant and requires good working knowledge of the particular plant. For this particular plant three controllers are deemed optimal. The controllers are designed by linearizing the plant at 25%, 35%, and 60% plant load. The reason for the concentration of controllers toward the lower operating range is the greater nonlinear dynamic behavior exhibited by plants at lower operating ranges. This is because the feedwater pump pressure and the throttle pressure are very sensitive to steam flow rate through headers and generator tubes when the flow is reduced during lower ranges of operation.

Since linear time-invariant approximations of the plant dynamics are used to design the controllers and the actual plant is nonlinear, the gain-scheduled control system is not likely to exhibit stability or performance over the entire operating range. However, all gain scheduling can still be implemented under the guidelines that the scheduling variables should vary slowly and capture the nonlinearities of the plant. For power plants plant load output/generated power output (MWe) is a scheduling variable that effectively captures the plant nonlinearities. Initial choice of generated power output was made keeping life extension in mind. Intuitively, slow variations in plant load reduce the damage in most plant components.

An important issue in gain scheduling involves the scheduling technique for the family of linear controllers. The choice is between smooth scheduling and switched scheduling. Smooth scheduling for wide-range control of large-order nonlinear plants is much more complicated because linearization of the high-order nonlinear plant dynamics makes the system poles and zeros far from each other at various operating points. Therefore, the linear controllers may be significantly dissimilar. The order of these controllers is very high (e.g., over 60 states). Any reduction in controller states to a lower order further diminishes any similarity between the individual controllers making smooth scheduling more difficult. Therefore, gain scheduling based on binary switching (i.e., switched scheduling) has been adopted.

Switched scheduling involves binary bidirectional switching from one controller to another with no intermediate stage. Successful implementation of the switching must not induce any abrupt changes (i.e., jerks) to the control system, while maintaining the required conditions of stability, performance, and life extension. These features satisfy the requirements of bumpless transfer (18). If the controller is observable, a simple observer-based technique used by Astrom et al. (19) and Graebe et al. (18) can be used for controller switching. The details of this technique are discussed by Kallappa and Ray (6).

Figure 6 shows the set-up used for the synthesis of the linear robust controller. The synthesis is based on a linearization of the nonlinear power plant model at a load of 25%, 35%, and 60% of the maximum load. Input multiplicative modeling uncertainty is represented by

$$W_{\mathrm{del}}(s) = 2\left(\frac{s+0.05}{s+1}\right) \tag{12}$$

which implies that the amount of plant uncertainty is being estimated as being 10% at low frequencies and 200% at high frequencies. This is because the plant model performance matches the steady-state plant operations very well; therefore, very little uncertainty is expected at lower frequencies. The disturbance weighting function is chosen to be

$$W_{\mathrm{dist}}(s) = \frac{0.1}{s+0.1} \tag{13}$$

which means that disturbances with frequency content of less than 0.1 rad/s are expected.

The physics of material degradation and operating experience lead to the observation that large oscillations of steam temperature and pressure are the major source of damage in power plant components, especially in the steam headers and steam generator tubes. Large oscillations in steam temperature may also cause high damage in the turbine blades, but the pressure oscillations are relatively less damaging. The rationale is that the structural damage is caused primarily by creep flow and thermal stresses leading to cracks. Creep is an exponential function of temperature and rapid temperature oscillations cause high thermal stresses and stress oscillations. On the other hand, unlike an exponential function, mechanical stress cycling induced by pressure oscillations is governed by a relatively less nonlinear relationship. Therefore pressure constraints are relaxed to enhance the quality of dynamic performance during load following. The dominant modes of thermal-hydraulic oscillations in a power plant are below 10 Hz (7). The amplitude of high-frequency oscillations (e.g., in the order of 10^2 Hz or more) of any output variables is likely to be insignificant. Therefore, a larger penalty is imposed on lower frequencies of each performance-weighting function. However, due to high-frequency unmodeled dynamics, the risk of completely ignoring high-frequency oscillations is nonnegligible, because rare as they might be, these incidents may cause instability, leading to catastrophic failures or unscheduled plant shutdown. Based on the above observations, each performance weight is formulated as the sum of a low-pass filter and an all-pass filter.

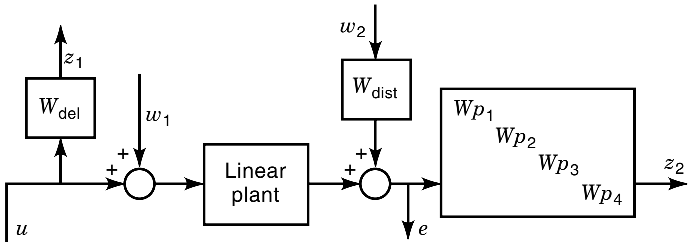

Figure 6. Synthesis of the linear robust feedback controller.

The main steam generator is the major source of thermal-hydraulic instability in once-through steam power plants where rapid variations in the length of the evaporator (e.g., two-phase water/steam region under subcritical conditions) section may occur due to changes in steam/water flow and rates of heat release. Any variations in the evaporator length are reflected in the main steam temperature (THS), which is the most significant of the damage-causing variables. Therefore, the penalty imposed on THS is most significant, that is, the low-pass filter has the largest bandwidth. The weights for the controller at 60% plant load are selected as follows:

$$\begin{aligned}
Wp_1(s) &= 20 + \frac{100}{s+5} \quad \text{for THS}\\
Wp_2(s) &= 20 + \frac{2}{s+0.1} \quad \text{for THR}\\
Wp_3(s) &= 10 + \frac{1}{s+0.1} \quad \text{for PHS}\\
Wp_2(s) &= 20 + \frac{2}{s+0.1} \quad \text{for JGN}
\end{aligned} \tag{14}$$

The performance weights for the controllers at 25% and 35% load impose a larger penalty on temperature oscillations because larger temperature variations are observed at lower load levels. This implies that the quality of dynamic performance is traded-off for better damage mitigation and stability. The performance weights for the controllers at 25% and 35% load are selected as follows:

$$\begin{aligned}
Wp_1(s) &= 30 + \frac{150}{s+5} \quad \text{for THS}\\
Wp_2(s) &= 30 + \frac{3}{s+0.1} \quad \text{for THR}\\
Wp_3(s) &= 10 + \frac{1}{s+0.1} \quad \text{for PHS}\\
Wp_2(s) &= 20 + \frac{2}{s+0.1} \quad \text{for JGN}
\end{aligned} \tag{15}$$

In each case, the generalized plant models (i.e., the augmentation of the linearized plant model with W_{del}, W_{dist} and W_p) have 47 states. The MATLAB μ-Analysis and Synthesis Toolbox was used to design a linear feedback controller using the method outlined above. The induced L_2 synthesis was performed through *D-K* iteration (8,15). The polynomial fits for D in the final iteration of all three controllers are of either order 3 or 4 and the stability robustness measure was below 0.8 for each controller. The controller at 60% has 71 states and each of the other controllers had 79 states. Most of these states are only lightly controllable and, after applying Hankel model order reduction, each controller is reduced to 26 states and the stability measure of each controller still remains below 0.8.

The implementation of the feedback control within the LELFC system is shown in Fig. 5. Both the feedforward and feedback control signals are discrete signals. The sequence of feedforward commands, $u^{ff}(k)$, is stored in a computer a priori, and the signal generated by the feedback controller, $\Delta u(k)$, is calculated by a computer on-line. At each sampling instant (e.g., every 0.1 s) the feedforward and feedback control signals are added together and converted into a continuous signal by using a zero-order hold device. Since the feedforward sequence is based on a 1 s sampling time, and the feedback sequence is based on a 0.1 s sampling time, each element in the feedforward sequence is applied for 10 consecutive 0.1 s samples. The error signal, $e(k)$, which serves as the input to the feedback controller, is calculated by subtracting samples taken from the plant outputs, $y(k)$, from the a priori chosen reference trajectory, $y^{ref}(k)$. Each of these signals are based on a 0.1 s sampling time.

SUPERVISORY SYSTEM

The supervisory system, as its name suggests, acts as an online supervisor. It has two major functions. The first function is to implement the gain scheduling of feedback controllers. This decision is made based on the sensor data, that is, the plant output, y. The second function is to select the reference signal y^{ref} based on the operation strategy and plant output. This decision is made using fuzzy logic and fuzzy membership functions (20). The supervisor is an expert system and is constructed based on expert knowledge of the plant and the structural damage models.

The gain-scheduling function of the supervisory controller can be incorporated into the feedback system too. If that is done, the feedback system can operate both with or without the supervisory system. This fact is used later on to test the superiority of fuzzy logic over a simple feedback system. The decision about y^{ref} using fuzzy logic is a function specific to the supervisor only. It requires as inputs plant load demand from the remote grid and plant output from the plant sensors and the output is y^{ref} (Fig. 2).

In order to emulate decision-making capabilities of a human supervisor, the supervisory system must be embedded with the knowledge of human operators. Yen et al. (21) have demonstrated the ability of fuzzy logic to emulate human supervisors. The basic configuration of the fuzzy controller is shown in Fig. 7. The nonfuzzy inputs are converted into fuzzy inputs via membership functions (20), in the fuzzifier. The membership function maps the nonfuzzy input to a real value in the interval 0 to 1, indicating the extent to which this input is a member of the fuzzy set. The fuzzy rule base is built upon expert knowledge of an experienced human operator in a rule-based format. The inference mechanism generates the output using the fuzzy input and the rule base. The defuzzifier converts the fuzzy output set into nonfuzzy analog or digital control signals. In this application, the fuzzy control algorithm serves to achieve three interrelated goals:

1. To maintain robust stability of the gain-scheduled control system through slow variations in the scheduling variable (plant load in MWe)
2. To avoid abrupt damage-inducing dynamic changes in plant variables during controller switching by enhancing smoothness of the switching mechanism
3. To reduce the damage rate in the critical plant components while satisfying the plant performance requirements, creating a trade-off between plant performance and damage during transients

The inputs to the supervisory controller have to be quantities that can be easily measured and are readily available, that is, sensor data $y(t)$. Similarly, its outputs must be quantities that an operator can manipulate to achieve the goals. Knowledge of the plant and damage dynamics helps in making these choices. Critical plant states and outputs which affect stability and structural damage should be inputs. The patterns and behavior of the outputs that lead to appreciable damage and instability should be incorporated into the membership functions and rule bases.

The critical nature of main steam temperature (THS) and hot reheat temperature (THR) in terms of damage and stability has been discussed earlier. In contrast, the other two plant outputs, main steam pressure (PHS) and generated load (JGN) are not as critical. Therefore, THS and THR are used to derive the inputs to the fuzzy controller. The effects of temperature can be critical in two ways. First, a rapid change in steam temperature may cause significant damage to the plant components or even plant instability. The rates of change of the two temperatures are therefore used as nonfuzzy inputs to the fuzzy controller. Even a slow change in temperature may lead to instability by gradually taking the controllers away from their region of attraction. To circumvent this problem, magnitudes of the two output temperature errors are also used as fuzzy inputs. Based on the fuzzy inputs, a

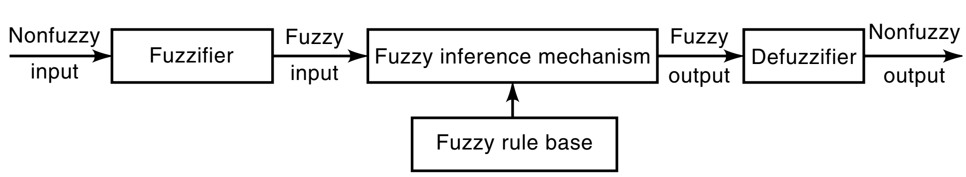

Figure 7. Fuzzy controller structure.

course of action is adopted, via an if–then rule base that partially captures human expertise. The nonfuzzy output of the fuzzy system is the load ramp rate which can be integrated to determine load—the gain scheduling variable. This choice provides a convenient means for achieving the first goal. The remaining two goals can also be achieved through this approach via judicious choice of the membership functions.

During transient operations the two temperatures THS and THR are major indicators of the damage-accumulation rates. In order to obtain better control of the damage-causing variables, slowing down of the process dynamics is the most natural action of the supervisory controller. This implies a reduction in the load ramp rate. On the other hand, a good temperature performance can leave sufficient margins to increase the ramp rate. This justifies the choice of the absolute value of ramp rate as the fuzzy controller output. For example, if the goal is to achieve a smooth load increase from 30% to 60% at the average rate of 10% full load per minute, the supervisor may decrease the ramp rate below 10% at certain points to maintain stability or reduce damage. On the other hand, if the sensor-based information indicates a low damage rate and stable operation, the load ramp rate can be safely increased.

The first step in the synthesis of a fuzzy control law is creating membership functions for the four inputs and one output. For the two temperature errors, identical membership functions are used because the process variables THS and THR are functionally similar. The same argument holds for the rates of change of these two temperatures. A third membership function is required for the output.

Each membership function set has cardinality of five. The membership functions are shown in Fig. 8. Unlike the membership functions of temperature rate and temperature error membership, functions of load ramp rate are not uniformly spaced. The spacing in load is arrived at via trial and error over extensive simulation runs, similar to what a human operator would like to do. The triangular shape of the membership functions is chosen for mathematical simplicity and produces sufficiently good results. An interpretation of these membership functions is as follows:

r_1 = very low rate of change of temperature
r_2 = low rate of change of temperature
r_3 = moderate rate of change of temperature
r_4 = high rate of change of temperature
r_5 = very high of change of temperature

Similar labels can be assigned to temperature error and load ramp rate. The membership functions are now combined into a set of fuzzy rules constituting a four-input single-output fuzzy control system with each input having cardinality of five. This implies that there can be 5^4 (=625) combinations of inputs and an if–then rule is required for each combination. To simplify this situation, the fuzzy control system is partitioned into two parallel processing fuzzy systems S_1 and S_2, as shown in Fig. 9. The inputs to S_1 are temperature rates and the output is the load ramp rate, while the inputs to S_2 are the temperature errors and output is also ramp rate. The junction "<" in Fig. 9 represents an operation which picks the minimum of the two outputs, that is, the slower ramp rate. Thus a conservative approach is adopted in order to simplify

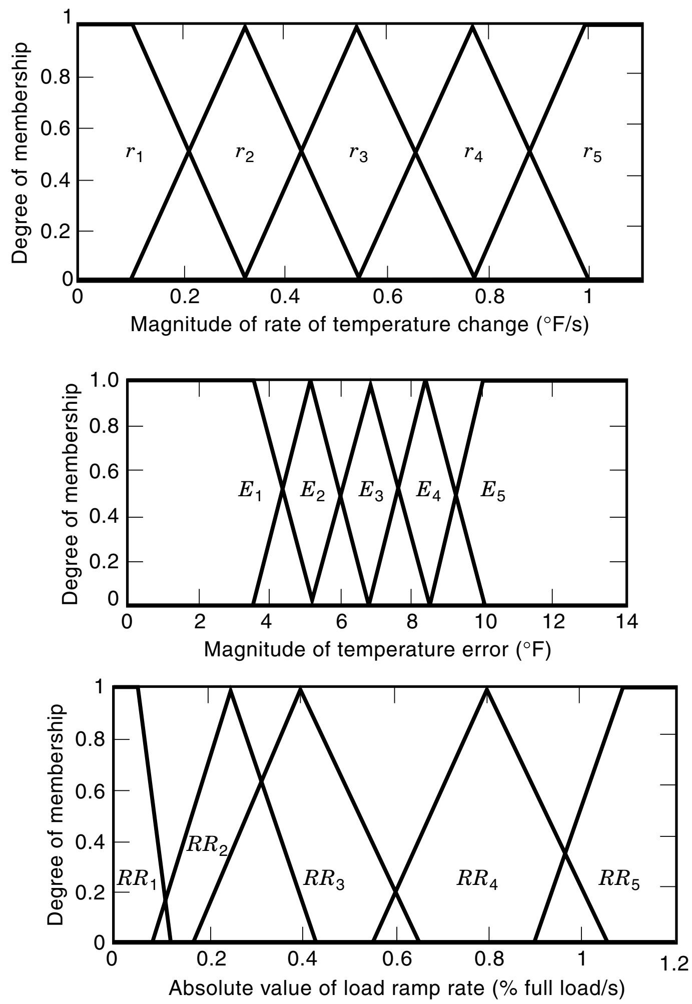

Figure 8. Membership functions.

a large rule base. The advantage of this simplification is that, instead of 625 rules, two sets of 25 if–then rules are now needed as listed in Table 1 and Table 2. For example, a rule *If* r_1^{THS} *and* r_1^{THR}, *then* RR_5 represents: *If the rate of change of main steam temperature is very low and the rate of change of hot reheat temperature is very low, then make ramp rate very high.*

The membership functions fuzzify the nonfuzzy inputs. The inference mechanism then determines the applicability of each rule to the present situation. The parameter λ_{ij}, determines the applicability of each of the 25 rules to the present situation and takes a value in [0, 1] representing a measure

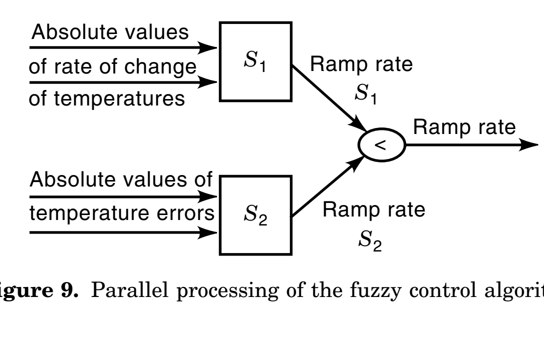

Figure 9. Parallel processing of the fuzzy control algorithm.

Table 1. If–Then Rules for Temperature Rate of Change (Fuzzy Controller S_1)

	r_1^{THS}	r_2^{THS}	r_3^{THS}	r_4^{THS}	r_5^{THS}
r_1^{THR}	RR_5	RR_4	RR_3	RR_2	RR_1
r_2^{THR}	RR_4	RR_4	RR_3	RR_2	RR_1
r_3^{THR}	RR_3	RR_3	RR_3	RR_2	RR_1
r_4^{THR}	RR_2	RR_2	RR_2	RR_2	RR_1
r_5^{THR}	RR_1	RR_1	RR_1	RR_1	RR_1

of the amount the inputs satisfy the *if* part of the respective rule. The subscripts i and j represent the row and column for rules. For example, in Table 1, $\lambda_{ij} = \min\{r_i^{\mathrm{THS}}, r_j^{\mathrm{THR}}\}$ implies that, λ_{ij} takes the minimum of the two values of the membership function involved in each rule.

The defuzzifier calculates one deterministic output in the form of ramp rate. The output is calculated as a weighted average of the outcome of each rule (RR_k, $k = 1, 2, 3, 4, 5$) with the respective λ's as the weights. Since there are no probabilities associated with the fuzzy decision-making in the present controller, each outcome is concentrated on the geometric mean (i.e., center of gravity) of its membership function. The membership functions in Fig. 8 are symmetric and the mean lies at the value with membership of one. Let the mean outcome of each rule be represented as $rr_{i,j}$, where $rr_{i,j}$ can take one of the five mean values, depending on the outcome of the *if–then* rule. Then, the final ramp rate is represented by:

$$\text{ramp rate} = \sum_{i,j=1\ldots5} \lambda_{ij} rr_{ij} \Big/ \sum_{i,j=1\ldots5} \lambda_{ij} \tag{16}$$

which is the weighted average of the geometric means of the output membership functions.

FEEDBACK-SUPERVISORY SYSTEM IMPLEMENTATION

The implementation strategy of the supervisory control system, shown in Fig. 10, has three main modules. The discrete-time and continuous time signals are denoted by "k" and "t", respectively, in parenthesis. The supervisory controller module consists of the gain scheduler and the fuzzy controller. The gain scheduling of controllers is carried out based on the measured plant outputs $y(k)$, specifically the fourth element of $y(k)$, which is the generated load (JGN) in MWe. However, the gain scheduling can also be implemented by the feedback module. Given a power plant operating strategy, the fuzzy-logic-based control module in the supervisory controller serves the role of generating $y^{\mathrm{ref}}(k)$. The feedforward signal is generated via equilibrium steady-state calculations. The robust feedback module is realized by three linear controllers whose ranges of operation are as follows:

1. Controller synthesized at 25% plant load: used for range [25%, 32%] plant load
2. Controller synthesized at 35% plant load: used for range (32%, 50%] plant load
3. Controller synthesized at 60% plant load: used for range (50%, 100%] plant load

All three controllers are synthesized closer to the lower end of their operating range. The rationale is that the extent of nonlinearity is much more severe as the load is diminished.

The sequence $u^{\mathrm{ff}}(k)$ of the feedforward signal is updated every 1 s by the fuzzy controller, based on $y^{\mathrm{ref}}(k)$, and is stored in the control computer a priori. The feedback control law $u^{\mathrm{fb}}(k)$ is generated on a 0.1 s sampling time and is implemented as discussed earlier.

The operating strategy simulated and tested here are load ramp-up and ramp-down. The first three elements, namely, reference signals for THS, THR, and PHS, of $y^{\mathrm{ref}}(k)$ are functions of the fourth element. Once the vector $\{\mathbf{yref}(k)\}$ is completely determined it can be used to generate feedforward input for the next instance. At any instant, one and only one linear controller is on-line and provides the feedback signal. The controller in use in Fig. 10 is the one synthesized at 25% plant load. While a single specific controller is on-line, the trackers for the remaining two controllers, which are off-line, are functioning to ensure that the controllers are ready to switch smoothly under a sudden change in the plant load demand. As soon as the active controller goes off-line, its tracker is switched on. While the main role of the supervisory controller is life extension without any significant loss of performance, it also ensures stability. It is shown in the next section via simulation experiments, that at times when the feedback controllers fail, the supervisory controller can maintain robust stability.

RESULTS AND DISCUSSION OF SIMULATION EXPERIMENTS

Simulation experiments are performed to demonstrate performance, robustness, and damage-mitigating capabilities of the entire control system for fossil power plants. This is accomplished by comparison of the plant dynamic performance under three control system configurations. Each control configuration uses the same feedforward policy. The first configuration uses just one feedback controller over the entire range of operation and no supervisory system. The second configuration uses the three gain scheduled controllers, but does not use the fuzzy functions of the supervisory controller. In effect, this is half the supervisory system without the intelligent fuzzy control function. The third configuration is the system depicted in Fig. 10, with the feedback system and the complete supervisory system. The goal of these simulations is to demonstrate the superiority of the combined feedback-supervisory system over the other two systems.

The comparison between these three cases is done based on output performance and structural damage. The plant performance requires generated plant load (JGN) to follow a predetermined trajectory. Each of the other three outputs, namely, THS, hot reheat temperature THR, and PHS, follow

Table 2. If–Then Rules for Temperature Error (Fuzzy Controller S_2)

	E_1^{THS}	E_2^{THS}	E_3^{THS}	E_4^{THS}	E_5^{THS}
E_1^{THR}	RR_5	RR_4	RR_3	RR_2	RR_1
E_2^{THR}	RR_4	RR_4	RR_3	RR_2	RR_1
E_3^{THR}	RR_3	RR_3	RR_3	RR_2	RR_1
E_4^{THR}	RR_2	RR_2	RR_2	RR_2	RR_1
E_5^{THR}	RR_1	RR_1	RR_1	RR_1	RR_1

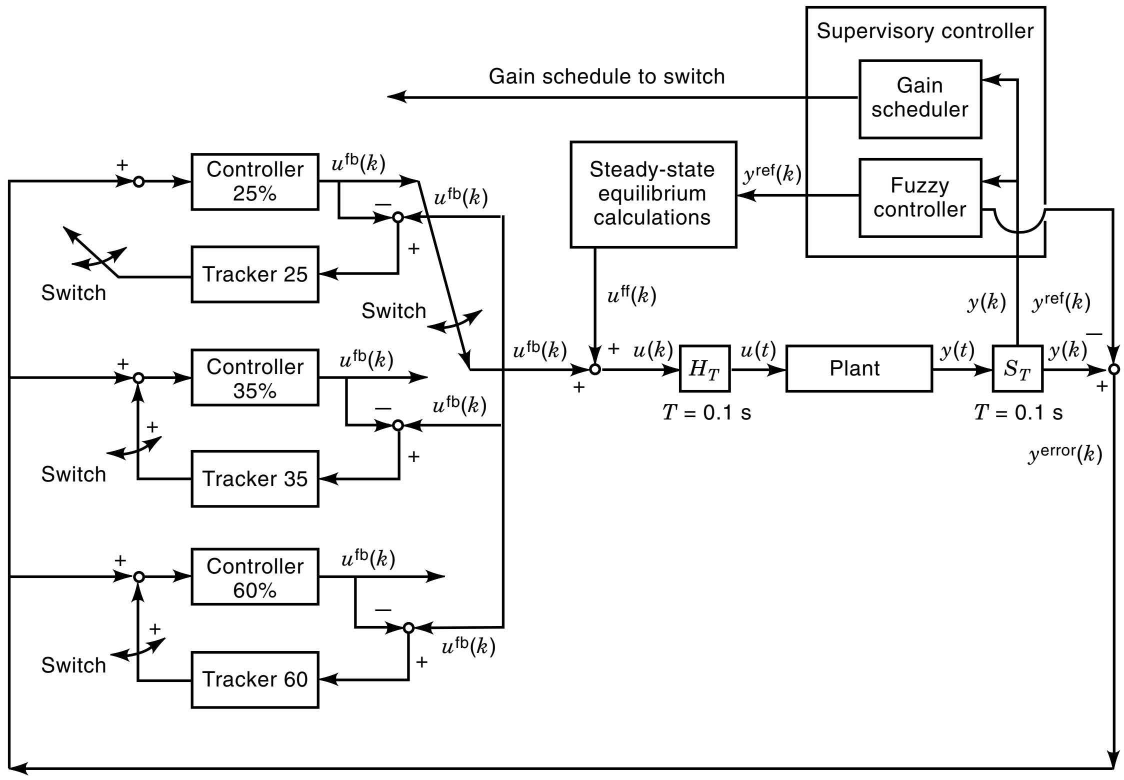

Figure 10. Implementation of supervisory control system.

a trajectory based on the current plant load and is maintained within respective bounds. During these operations, damage accumulation in the main steam header, hot reheat header, and superheater tubes is calculated using the damage prediction system of Fig. 1. Simulation experiments are also performed to test the robustness of the control system under plant transients. Some of the plant parameters, like time constants of valve dynamics, heat transfer coefficients, and turbine and pump efficiencies, are perturbed and the outputs and damage accumulation are compared for the three cases.

SIMULATION SET-UP

To test the closed-loop control system, for both nominal and perturbed plant conditions (two operations): a power ramp-up from 25% to 100% plant load and a power ramp-down from 100% to 25% plant load, are simulated. The recommended ramp rate is 10% per minute for both operations. The desired operating conditions for the THS, THR, and PHS at a given plant load (JGN) are a function of the JGN. The operating conditions are determined as the steady-state values of these outputs at the given plant load. The operating conditions for each load are as follows:

- 25% load—[THS, THR, PHS] = [935°F, 990°F, 2050 psi]
- 30% load—[THS, THR, PHS] = [948°F, 998°F, 2285 psi]
- 40% to 100% load—[THS, THR, PHS] = [950°F, 1000°F, 2415 psi]

Linear interpolation determines the output values in between these conditions. At loads below the 40% power level the pressure PHS needs to be decreased to avoid feedwater pump valve saturation. The feedwater pump is primarily responsible for generating the steam pressure. The operating temperatures are also lowered slightly for thermodynamic reasons. It should be noted that the reference trajectories for these three operating conditions are a function of the actual load output and not load demand.

The damage accumulation and rates are monitored for three critical components. The main steam header, which damages from fatigue cracking and thickness reduction due to creep. Maximum crack growth occurs on the outer surface and in the radial direction. An initial value of crack length is assumed. Normalized creep is calculated as the reduction in header thickness per unit original thickness and is designated "Creep Thinning". The hot reheat header and superheater tubes are the other two components. Damage in each of these is predominantly due to creep and is represented in a fashion identical to the creep damage in the main steam header. Each of these assumed to be made of $2\frac{1}{4}$% chromium and 1% molybednum ferritic steel.

The next two subsections present simulation results for nominal and perturbed plant conditions. Each set of simulation experiments is performed by running the feedback-supervisor control system first. The time taken to complete the operation using this system is used for the other two systems. This ensures a proper comparison of the performance and damage mitigation among the various control systems. The plots in the figures are marked with appropriate labels (e.g., "single controller", "gain sch." for gain scheduled, and "feedback-sup." for feedback-supervisor) to indicate different configurations.

SIMULATION UNDER NOMINAL CONDITIONS

For nominal plant simulation results from only ramp-up operations are reported. Three different configurations of feedback control are used as mentioned earlier. The single robust controller, adopted for simulation experiments, yields the best performance out of many single controllers that are designed and tested. This controller is an induced L_2 controller based on the plant model linearized at 40% full load. Figure 11 shows the performance of this controller for ramp-up operations. The average ramp rate is determined from the time taken to ramp the feedback-supervisory system. It takes 738 s for the ramp-up operation with an average ramp rate of 6.1% (of full load) (see Fig. 12). The plots in Fig. 12 show the

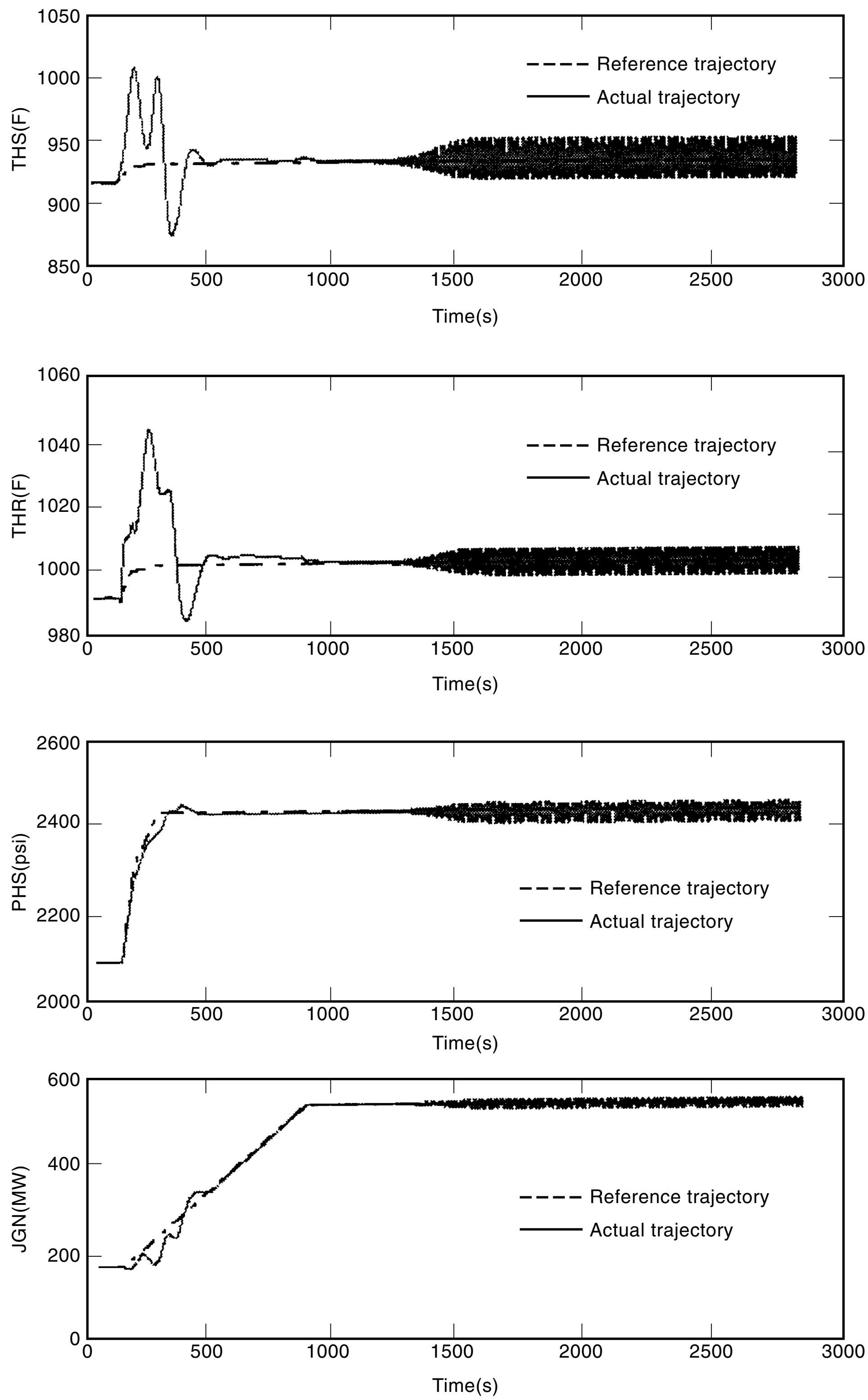

Figure 11. Ramp-up performance of single controller for nominal plant. Power ramp up takes place from 25% to 100% plant load, starting at 100 s and lasting for 738 s. The single feedback controller causes large oscillations in temperatures and power output during both transient and steady state operations.

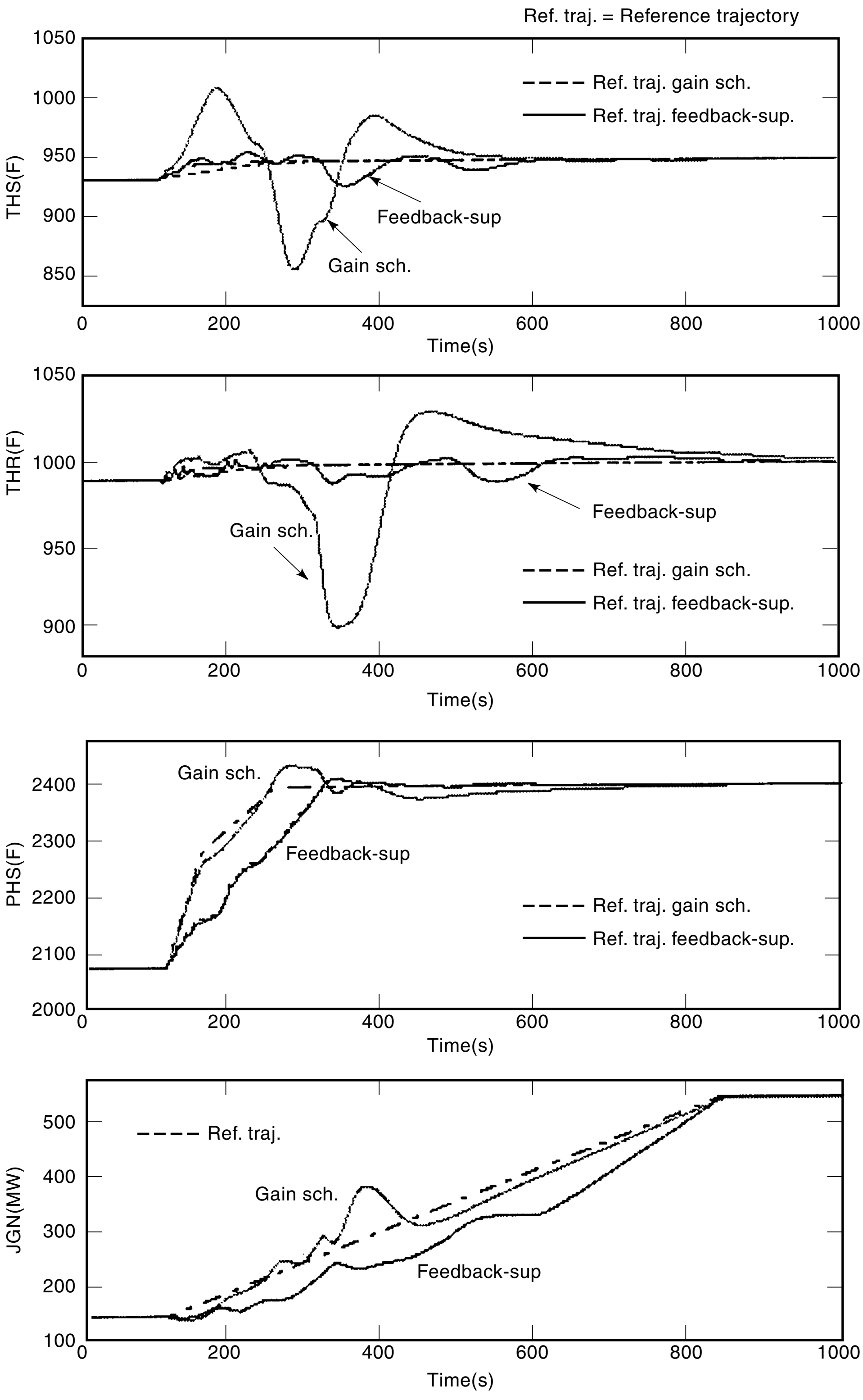

Figure 12. Ramp-up performance for the nominal plant. Power ramp up takes place from 25% to 100% plant load, starting at 100 s and lasting for 738 s. The gain-scheduled feedback controller causes larger oscillations in temperatures and power output during transient operations.

respective initial steady-state loads held for the first 100 s, to demonstrate absence of any initial (nonsteady-state) transients. Similarly, the final steady states are held for an extended period of time to exhibit stability. Referring back to the single controller case in Fig. 11, the main steam temperature (THS) abruptly increases by about 100°F as the power ramp-up starts, and the hot reheat steam temperature (THR) by over 55°F. Sudden temperature changes of this nature may cause structural damage to the steam headers as well as in the steam turbines. The final steady-state responses are extremely oscillatory for all four outputs in Fig. 11. This is highly undesirable for both dynamic performance and structural damage. It is reiterated that this single controller has yielded the best performance out of a large group of single robust controllers that were designed. It is also found to be unstable for injected plant perturbations.

Figure 12 shows comparisons of the outputs between "gain scheduled" (i.e., without fuzzy logic) and "feedback-sup.", under ramp-up. The reference trajectories ("Ref. Tra.") for THS, THR, and PHS are different for the two cases because they are determined by the current load output (JGN) and at any instance JGN can differ for either case. Gain scheduling shows a marked improvement over "single controller" system in terms of steady-state behavior but the transient response still has large temperature variations almost like the "single controller" in Fig. 11. In contrast, the "feedback-sup." outputs show excellent behavior for the steam temperature and pressure transients, THS, THR, and PHS, that are directly responsible for damage reduction. Unlike the other two control systems, the temperature variations are well controlled.

For ramp-up operations in Figs. 11 and 12, the load-following performance of all three scenarios is comparable. The "single controller" has slight oscillations, the "gain scheduled" controller suffers from large transients around the points of controller switching especially at 50% load, and the feedback-supervisory system stays below the reference trajectory until the end. However, the other three outputs, PHS, THS, and THR, are superior for the feedback-supervisory system. The load-following performance can be improved by changing the frequency-dependent performance weights W_p in the robust feedback controller synthesis as and by allowing larger ramp rates in the membership functions of the plant outputs. For each case, the changes involve a trade-off, which is the designers' decision.

Figure 13 compares the damage under a ramp-up operation. The operation is preceded by 1000 s of steady-state and followed by another 2000 s. This ensures that any delayed dynamics in damage will show up during steady-state operation. In Fig. 13, for each of the critical components, the feedback-supervisory system yields better damage control. Maximum damage reduction takes place in the main steam header, because it is a thick pipe and is more prone to thermal stresses arising from larger temperature gradients across the wall. The control system focuses on reduction of temperature and pressure fluctuations in the main steam header. The hot reheat header, on the other hand, is a thinner pipe and its damage is mainly due to the temperature and not temperature gradients. A similar logic applies to the superheater tubes, which are not as thick as the main steam header. For superheater and other steam generator tubes, the main cause of damage is the fireball size in the furnace, which is primarily responsible for transfer of (radiant) thermal energy to the tubes. The fireball size is controlled by the air-fuel valve. Under nominal plant operations, the feedforward control input to this valve is carefully designed to avoid any sudden change in fireball size and the feedback signal is responsible for fine-tuning only. It will be shown later that under perturbations there is vast improvement in damage mitigation and stability can be achieved by using the feedback-supervisory system. In conclusion, during power ramp-up, the "single controller" yields better life extension of the steam generator tubes than the "gain scheduled controller," but the "feedback-sup." is the best amongst the three controllers. Similar trends were noticed for ramp-down operation, except that the single controller gave highest damage and the worst performance. The results for nominal plant power ramp-up operation are summarized in Table 3.

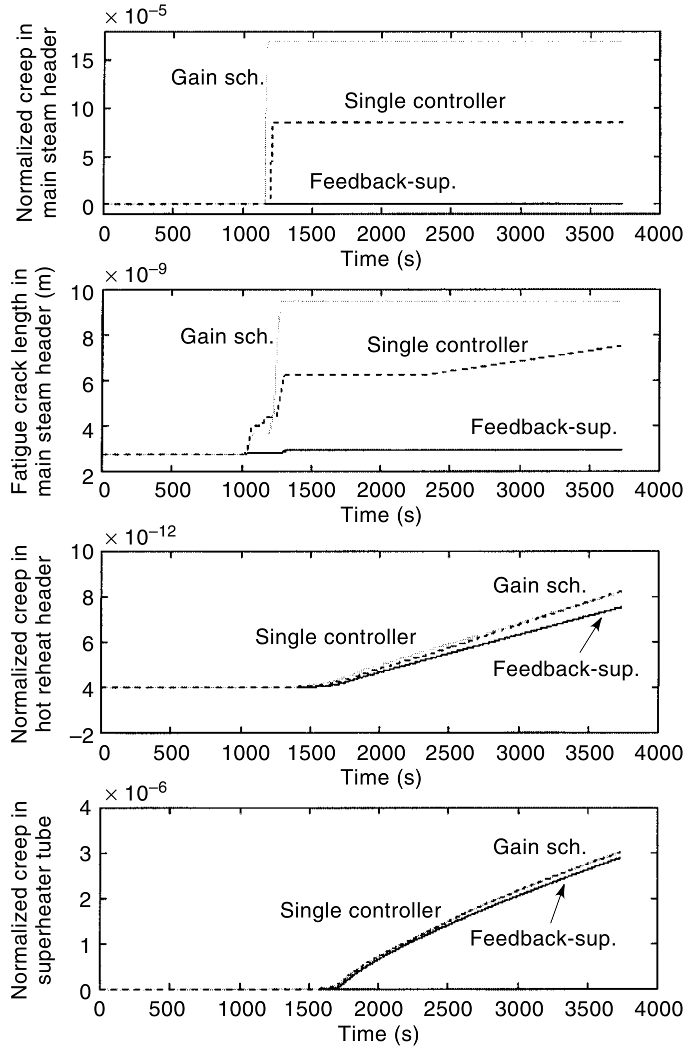

Figure 13. Damage during ramp-up operation in nominal plant.

PERTURBED PLANT SIMULATION

Simulation experiments are also conducted on the plant model with injected perturbations, in order to test the robustness of the control system. The following perturbations were introduced:

- 3% decrease in the efficiencies of the turbines and feedwater pump turbines and feedwater pumps due to structural degradation of rotating components
- 3% decrease in the heat transfer coefficients in the steam generator and reheater tubes resulting from possible scale formation on the inside wall
- 25% increase in the time constants of the governor, feedpump turbine, and fuel/air valves due to possible degradation of the actuator components

The "single controller" was unstable under perturbed conditions for both ramp-up and ramp-down and these results

Table 3. Summary of Results for Power Ramp Up Operation in Nominal Plant

		Performance		
Feedback Type/Attribute	Stable	Steady State	Transient	Damage Mitigation
Single Controller	Yes	Poor	Fair	Poor
Gain-Scheduled	Yes	Fair	Fair	Very Poor
Feedback-Supervisor	Yes	Good	Good	Good

Legent: NA = Not Available.

are not shown. Figure 14 has the ramp-down outputs for the perturbed plant under gain-scheduled and the feedback-supervisor system. There is a trade-off between power ramp-rate and temperature control at lower loads where steam temperatures begin to oscillate. However, the improvement in performance by using the feedback-supervisor system is evident, especially in the case of THS. Figure 15 shows the damage for both controllers. Similar to the results in Fig. 13, the damage is less for the feedback-supervisor system. But, unlike Fig. 13, there is a marked improvement in damage control for superheater tubes. This is because, as mentioned in the previous section, damage mitigation is largely accomplished by the feedforward action for the nominal plant. In contrast, for the perturbed plant, the feedforward action is no longer accurate and consequently the feedback action plays a relatively larger role. Thus, during ramp-down, for the perturbed plant, the feedback-supervisor system yields both better performance and damage control than the gain scheduled system, with a trade-off in load rate. These results are tabulated in Table 4.

Figure 16 shows the ramp-up operation for the perturbed plant. While the feedback-supervisor system performs reasonably well, the control system becomes unstable without the fuzzy controller. The rationale for this observation is as fol-

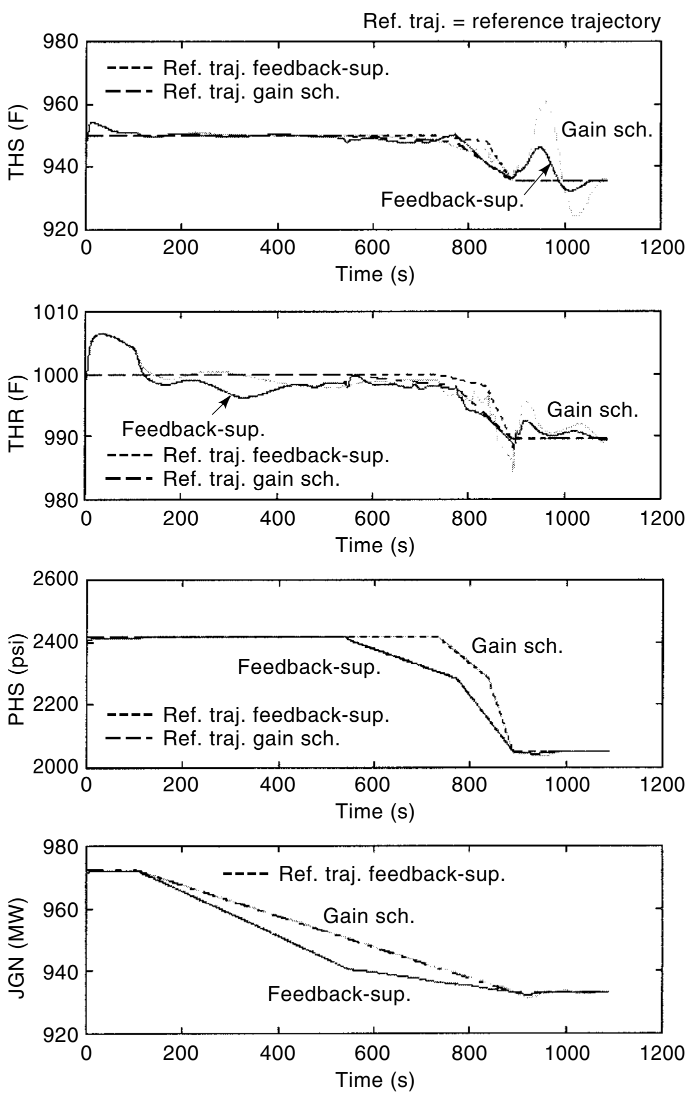

Figure 14. Ramp-down performance for perturbed plant.

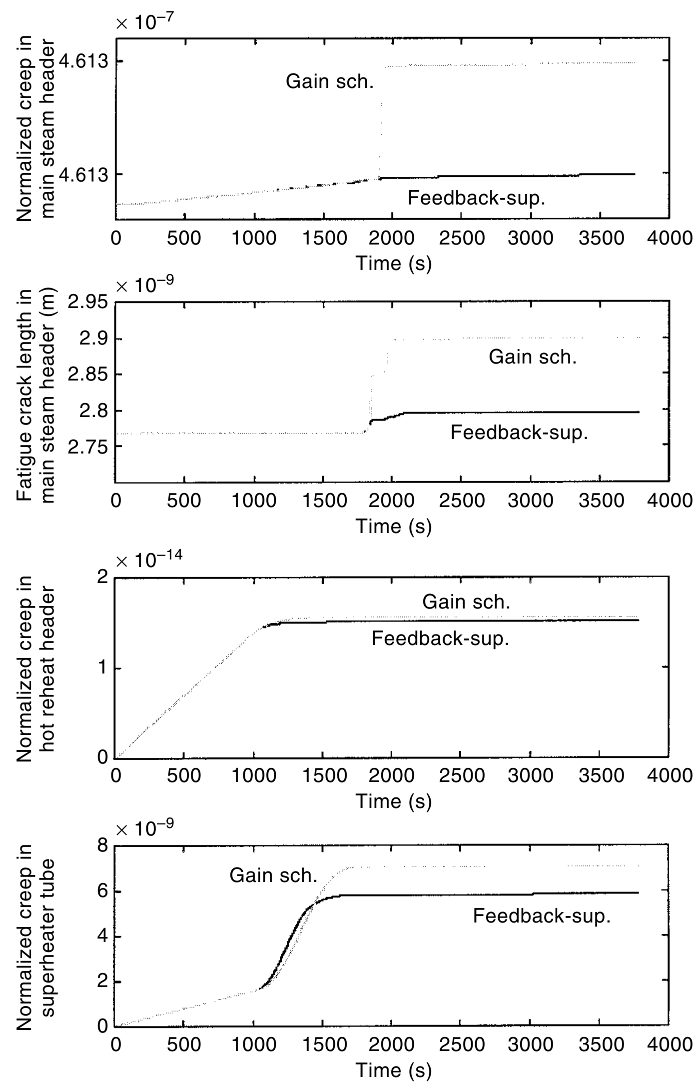

Figure 15. Damage during ramp-down in perturbed plant.

Table 4. Summary of Results for Power Ramp Down Operation in Perturbed Plant

		Performance		
Feedback Type/Attribute	Stable	Steady State	Transient	Damage Mitigation
Single Controller	No	NA	NA	NA
Gain-Scheduled	Yes	Fair	Fair	Fair
Feedback-Supervisor	Yes	Good	Good	Good

NA = Not Available

lows: As the system starts to move away from the reference points, the fuzzy controller slows down the ramp rate and thereby the rate of change of the plant load is reduced and stability is maintained. This is in accordance with the claim that a slow variation of the gain scheduling variable, in this case the plant load, ensures stability. This observation clearly demonstrates the effectiveness of fuzzy logic in keeping the control system robust. Since, for this case, all other systems are unstable, no damage comparisons are made (Table 5).

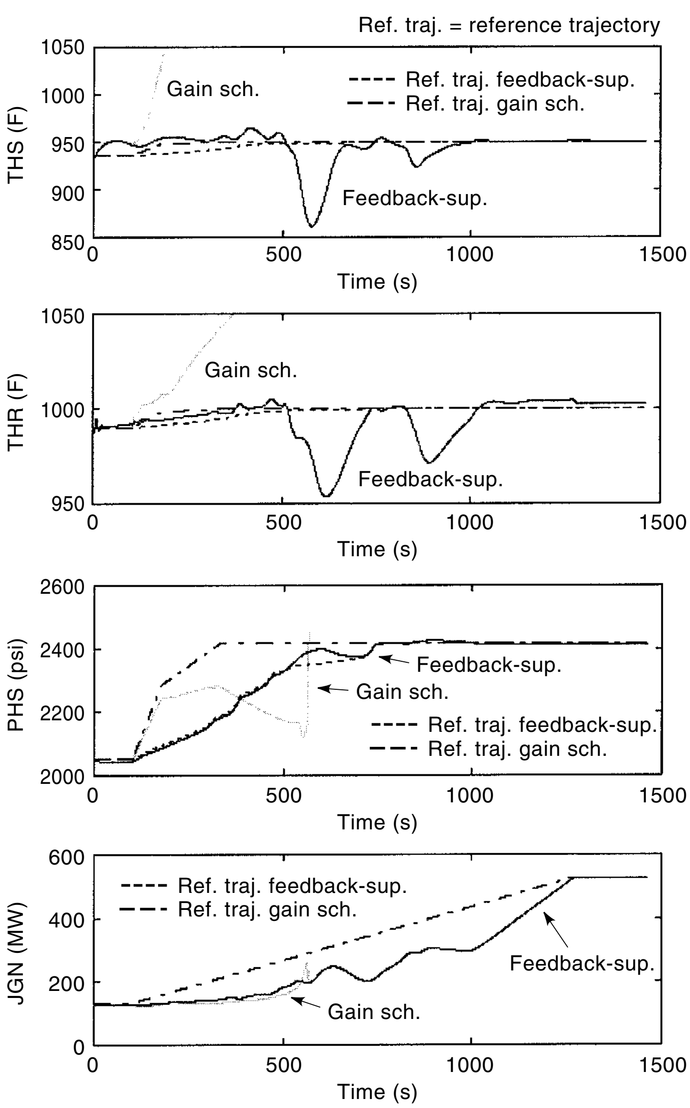

Figure 16. Ramp-up performance of perturbed plant.

CONCLUSIONS

This article presents three distinct tools for power plant load control where the objectives are to enhance load-following and load regulation in power plants with an emphasis on life extension and trade-off between plant performance and component life. These three tools, namely, optimal feedforward, gain-scheduled linear feedback, and supervisory control using fuzzy logic, can be used in conjunction with each other or independently to form a life-extending load-following control (LELFC) system for power plants. The LELFC systems are synthesized assuming that the designer has a thorough knowledge and understanding of the functioning of power plants. The importance of each of these techniques has been discussed earlier. An important feature of these systems is the ease of synthesis and implementation. All of the above system synthesis can be carried out using simple workstations and fast PCs. On-line software implementation of these systems can be done using personal computers. While the feedback controllers are not flexible, the supervisory controller can be adjusted and changed on-line during operation to suit any change in demand or other operating conditions.

Simulation runs have been conducted to test the dynamic performance versus damage mitigation trade-off of the LELFC systems under load-following operations. The feedforward system achieves significant improvement in damage mitigation with almost no loss in the load-following capability. However, it must be remembered that the feedforward is not robust and can be used only under certain conditions. Based on the results of simulation experiments, it is apparent that there is practically no trade-off in damage control among the major critical components of the power plant. It also establishes the overall superiority of gain scheduling with fuzzy control. This concept of wide-range life-extending load following is of significant engineering importance. For example, including damage in the control scheme leads to potential life extension of the plant as well as increasing the mean time between major maintenance actions.

Feedforward optimization is dependent on availability of accurate mathematical models of the power plant and structural damage of the critical components. Adequate computational resources are needed for fast convergence of an optimal solution. For its implementation, load demand has to be known a priori. The induced L_2-norm technique, used for controller synthesis, can be replaced by other techniques, but the performance constraints and criteria should remain the same. The number of gain-scheduled controllers can vary from plant to plant and this decision requires working knowledge of the plant operations.

The supervisory system with fuzzy logic improves the load-following capabilities of the system. The fuzzy logic based sys-

Table 5. Summary of Results for Power Ramp Up Operation in Perturbed Plant

Feedback Type/Attribute	Stable	Performance Steady State	Transient	Damage Mitigation
Single Controller	No	NA	NA	NA
Gain-Scheduled	No	NA	NA	NA
Feedback-Supervisor	Yes	Good	Good	Not Calculated

NA = Not Available

tem is very flexible especially in terms of the membership functions. The temperature membership functions can be adjusted to reduce damage or relax damage constraints in order to improve performance. The output membership functions of load ramp rate can be a function of load demand, instead of keeping them fixed. This is an important issue and should be further investigated.

BIBLIOGRAPHY

1. S. C. Stultz and J. B. Kitto (eds.), *Steam / Its Generation and Use.* 40th ed., Barberton, OH: Babcock & Wilcox, 1992.
2. A. Ray et al., Damage-mitigating control of mechanical systems: Part I—Conceptual development and model formulation, *ASME J. Dynamic Syst., Meas. Control,* **116** (3): 437–447, 1994.
3. A. Ray et al., Damage-mitigating control of mechanical systems: Part II—Formulation of an optimal policy and simulation, *ASME J. Dynamic Syst., Meas. Control,* **116** (3): 448–455, 1994.
4. X. Dai and A. Ray, Life prediction of the thrust chamber wall of a reusable rocket engine, *AIAA J. Propulsion Power,* **11** (6): 1279–1287, 1995.
5. P. Kallappa, M. S. Holmes, and A. Ray, Life-extending control of fossil fuel power plants, *Automatica,* **33** (6): 1101–1118, 1997.
6. P. Kallappa and A. Ray, Fuzzy Wide-Range Control of Fossil Power Plants for Life Extension and Robust Performance, *IEEE Conf. Decision Controls,* Tampa, FL, 1998.
7. C-K. Weng, A. Ray, and X. Dai, Modeling of power plant dynamics and uncertainties for robust control synthesis, *Appl. Math Modeling,* **20**: 501–512, 1996.
8. K. Zhou, J. C. Doyle, and K. Glover, *Robust and Optimal Control,* Upper Saddle River, NJ: Prentice-Hall, 1996.
9. *Remaining Life Assessment of Superheater and Reheater Tubes,* EPRI CS-5564, Project 2253-5, Final Report, May, 1988.
10. M. Lele, A. Ray, and P. Kallappa, Life Extension of Superheater Tubes in Fossil Power Plants, *ISA 96 POWID Conf.,* Chicago, IL, 1996.
11. *Creep Fatigue Pro: On Line Creep-Fatigue Damage and Crack Growth Monitoring System,* EPRI TR 100907, Project 1893-11, Final Report, July, 1992.
12. J. S. Shamma and M. Athans, Analysis of gain scheduled control for nonlinear plants, *IEEE Trans. Autom. Control,* **35**: 890–907, 1990.
13. J. C. Doyle et al., State-space solutions to standard H_2 and H- control problems, *IEEE Trans. Autom. Control,* **AC-34**: 831–847, 1989.
14. B. A. Bamieh and J. B. Pearson, Jr., A general framework for linear periodic systems with applications to H_∞ sampled data control, *IEEE Trans. Autom. Cont.,* **37**: 418–435, 1992.
15. G. J. Balas et al., *μ-analysis and Synthesis Toolbox for use with MATLAB,* Natick, MA: Math Works, 1995.
16. N. Sivashankar and P. P. Khargonekar, Robust stability and performance analysis of sampled-data systems, *IEEE Trans. Autom. Control,* **38**: 58–69, 1993.
17. W. J. Rugh, Analytical framework for gain scheduling, *IEEE Control Syst. Mag.,* **11** (1): 79–84, 1991.
18. S. F. Graebe and A. L. B. Ahlen, Dynamic transfer among alternative controllers and its relation to antiwindup controller design, *IEEE Trans. Control Syst. Technol.,* **4**: 92–99, 1996.
19. K. J. Astrom and B. Wittenmark, *Computer Controlled Systems: Theory and Design,* Englewood Cliffs, NJ: Prentice-Hall, 1984.
20. M. Jamshidi, N. Vadiee, and T. J. Ross (eds.), *Fuzzy Logic and Control,* 1st ed., Englewood Cliffs, NJ: Prentice-Hall, 1993.
21. J. Yen, R. Langari, and L. A. Zadeh, *Industrial Applications of Fuzzy Logic and Intelligent Systems,* Piscataway, NJ: IEEE Press, 1995.

PATTADA KALLAPPA
ASOK RAY
Pennsylvania State University